Observation of a new high-spin isomer in ^{94}Pd

T. S. Brock,[1] B. S. Nara Singh,[1] P. Boutachkov,[2] N. Braun,[3] A. Blazhev,[3] Z. Liu,[4] R. Wadsworth,[1] M. Górska,[2] H. Grawe,[2]
S. Pietri,[2] C. Domingo-Pardo,[2] D. Rudolph,[5] S. J. Steer,[6] A. Ataç,[7] L. Bettermann,[3] L. Cáceres,[2] T. Engert,[2] K. Eppinger,[8]
T. Faestermann,[8] F. Farinon,[2] F. Finke,[3] K. Geibel,[3] J. Gerl,[2] R. Gernhäuser,[8] N. Goel,[2] A. Gottardo,[4] J. Grębosz,[9] C. Hinke,[8]
R. Hoischen,[2,5] G. Ilie,[3] H. Iwasaki,[3] J. Jolie,[3] A. Kaşkaş,[7] I. Kojuharov,[2] R. Krücken,[8] N. Kurz,[2] E. Merchán,[10] C. Nociforo,[2]
J. Nyberg,[11] M. Pfützner,[12] A. Prochazka,[2] Zs. Podolyák,[6] P. H. Regan,[6] P. Reiter,[3] S. Rinta-Antila,[13] H. Schaffner,[2] C. Scholl,[3]
P.-A. Söderström,[11] N. Warr,[3] H. Weick,[2] H.-J. Wollersheim,[14] and P. J. Woods[4]

(RISING Collaboration)

[1]*Department of Physics, University of York, York YO10 5DD, United Kingdom*
[2]*GSI, D-64291 Darmstadt, Germany*
[3]*IKP, Universität zu Köln, D-50937 Köln, Germany*
[4]*School of Physics and Astronomy, University of Edinburgh, Edinburgh, United Kingdom*
[5]*Department of Physics, Lund University, S-22100 Lund, Sweden*
[6]*Department of Physics, University of Surrey, Guildford, Surrey GU2 7XH, United Kingdom*
[7]*Department of Physics, Ankara University, 06100 Tandoğan, Ankara, Turkey*
[8]*Physik Department E12, Technische Universität München, D-85748 Garching, Germany*
[9]*The Institute of Nuclear Physics PAN, Kraków, Poland*
[10]*Departamento de Física, Universidad Nacional de Colombia, Bogotá, Colombia*
[11]*Department of Physics and Astronomy, Uppsala University, SE-75120 Uppsala, Sweden*
[12]*IEP, Warsaw University, PL-00-681 Warsaw, Poland*
[13]*Department of Physics, Oliver Lodge Laboratory, University of Liverpool, Liverpool L69 7ZE, United Kingdom*
[14]*GGSI, D-64291 Darmstadt, Germany*

A second γ-decaying high-spin isomeric state, with a half-life of 197(22)ns, has been identified in the $N = Z + 2$ nuclide ^{94}Pd as part of a stopped-beam Rare Isotope Spectroscopic INvestigation at GSI (RISING) experiment. Weisskopf estimates were used to establish a tentative spin/parity of 19^-, corresponding to the maximum possible spin of a negative parity state in the restricted ($p_{1/2}$, $g_{9/2}$) model space of empirical shell model calculations. The reproduction of the $E3$ decay properties of the isomer required an extension of the model space to include the $f_{5/2}$ and $p_{3/2}$ orbitals using the CD-Bonn potential. This is the first time that such an extension has been required for a high-spin isomer in the vicinity of ^{100}Sn and reveals the importance of such orbits for understanding the decay properties of high-spin isomers in this region. However, despite the need for the extended model space for the $E3$ decay, the dominant configuration for the 19^- state remains $(\pi p_{1/2}^{-1} g_{9/2}^{-3})_{11} \otimes (\nu g_{9/2}^{-2})_8$. The half-life of the known, 14^+, isomer was remeasured and yielded a value of 499(13) ns.

The $N \approx Z$ nuclei just below ^{100}Sn are of particular interest in contemporary nuclear structure studies. As well as lying on the pathway for rp-process nucleosynthesis in x-ray burster scenarios [1], these nuclei also provide significant information in relation to shell structure close to the last doubly magic $N = Z$ nuclide [2] and constitute a key region for testing the reliability of the shell model (SM) and SM interactions [3]. The region is generally well described by the SM in a minimum space comprising $p_{1/2}$ and $g_{9/2}$ protons and neutrons [3–5]. Exploration of the limits of this approach with respect to inclusion of the $p_{3/2}$ and $f_{5/2}$ orbitals and excitations across the $N = Z = 50$ shell closure is a challenge both to the SM and experimental techniques.

This region is also remarkable for an abundance of isomeric states [6]. Particularly interesting is the occurrence of high-spin isomers which can provide an ideal testing ground for the study of neutron-proton interactions near the $N = Z$ line [6]. One of the most striking cases is the (21^+) level in ^{94}Ag, with recent papers reporting evidence for a variety of particle decay channels: β [7,8], βp [9], p [10], and $2p$ [11]. The latter of these is the subject of much debate in the literature [12–16].

The $T_z = 1$ nuclide ^{94}Pd has been studied in a number of experiments [7,8,17–21] and has a known 14^+ isomer that decays through γ decay and internal conversion (IC). The half-life of this state has been measured previously, yielding values of 800(200) [17], 600(100) [18], 530(10) [19], and 468(19) [21] ns. A cascade of transitions above the 14^+ isomer has been tentatively placed from β-decay studies of the (21^+) isomer in ^{94}Ag [7,8]. The current work presents data from a Rare Isotope Spectroscopic INvestigation at GSI (RISING) experiment showing clear evidence of a second isomeric state that feeds the 14^+ level through some of these transitions. The reproduction of the decay properties of this isomer in shell-model calculations requires the inclusion of the negative-parity $p_{3/2}$ and $f_{5/2}$ orbitals.

^{94}Pd and other nuclei of interest were produced by the fragmentation of an 850 MeV/nucleon ^{124}Xe beam, provided by the SIS synchrotron at GSI, on a 4 g/cm^2 ^{9}Be target.
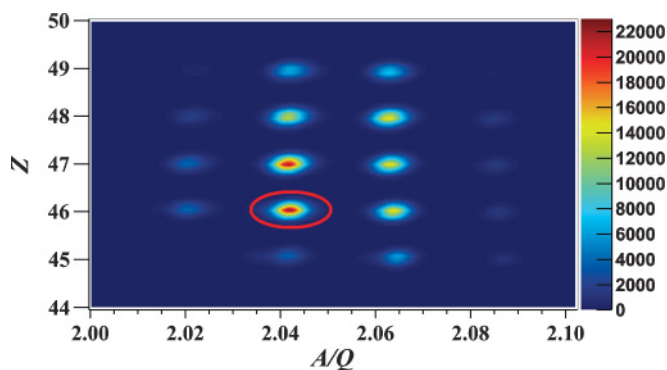
FIG. 1. (Color online) Fragment identification plot. The ^{94}Pd ions are ringed. The intensity color scale is given to the right.

Fragments were separated by the FRagment Separator (FRS) (see Ref. [22] and Fig. 1 of Ref [21]) and detectors at the central, "S2," and final, "S4," foci were used to uniquely identify each ion on an event-by-event basis as described in Refs. [21,23] with the addition of time projection chambers at each focal plane for more precise position measurements. Figure 1 shows a Z versus A/Q identification plot using the data from the FRS detectors. Due to the high energies involved, in virtually all cases the ions are fully stripped, i.e., $Q = Z$.

At the S4 focal plane the transported fragments were slowed down in an aluminum degrader, passed through a further scintillator, allowing for rejection of ions that underwent nuclear reactions in the degrader, and implanted in an active stopper. The stopper consisted of nine double-sided silicon strip detectors (DSSSD) arranged in three layers of three detectors, with each layer facing normal to the beam axis. A description of the properties of a similar, six DSSSD, stopper is given in Ref. [24]. The stopper was surrounded by the RISING
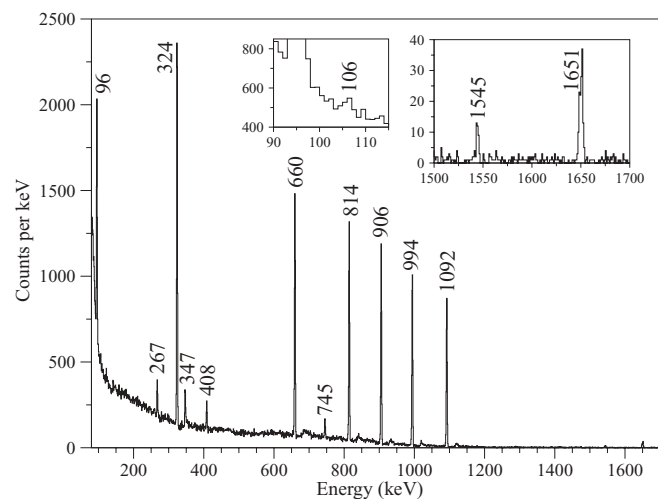

FIG. 2. Energy spectrum gated on ^{94}Pd ions. The seven largest peaks correspond to the yrast transitions from the 14^+ isomer to the ground state. The peaks at 347 and 745 keV are also from below the 14^+ isomer, but the peaks at 267 and 408 keV emanate from levels above it. The right inset shows peaks at 1545 and 1651 keV, while the left inset shows weak evidence of a 106 keV transition.
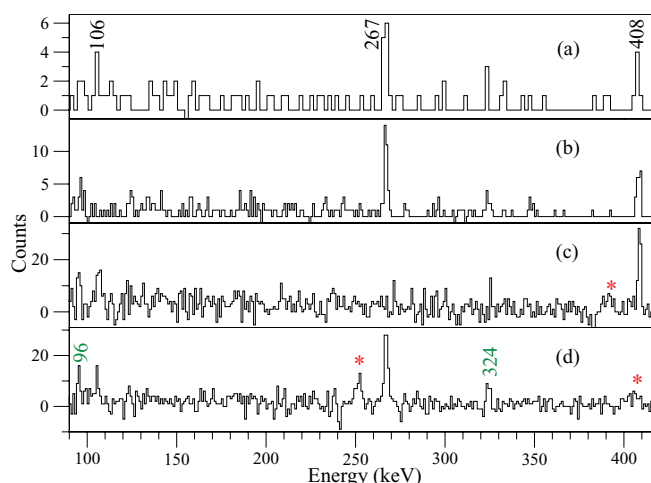

FIG. 3. (Color online) Prompt coincidences for the (a) 1545, (b) 1651, (c) 267, and (d) 408 keV transitions. (a) is 2 keV per bin and (b)–(d) are 1 keV per bin. Peaks corresponding to transitions below the 14^+ isomer can be seen due to the 250 ns width of the coincidence window. Peaks marked with "*" sum with the gating energy to 660 or 814 keV and are thus attributed to Compton scattering.

array of 105 germanium (Ge) detectors in its stopped beam configuration [23]. Using the information from the S2 and S4 detectors and the energy and timing information from the Ge detectors, time-walk corrected γ-time and γ-γ matrices were constructed for each implanted nuclide. The data were analyzed in ROOT [25] and RADWARE [26], and half-lives were determined using the ROOT implementation of MINUIT [27].

The S4 degrader has a detrimental effect on isomer spectroscopy due to bremsstrahlung radiation associated with the slowing down of the ions as they pass through [28]. This leads to spurious counts in the γ-ray spectra: the "prompt flash." Spectroscopic studies of low-energy transitions from short-lived isomers are particularly badly affected due to the (orders of magnitude) larger contribution the flash makes at lower energies (especially below $\sim$150 keV in the present case) and the poorer time resolution at such energies which smears the flash out over a number of time bins.

Figure 2 shows a projection to the energy axis of the γ-time matrix associated with ^{94}Pd implantation events. Defining $t = 0$ as the time at which the prompt flash peaks, the time range of the projection corresponds to $t = 175$ to $t = 1025$ ns. The yrast transitions from 14^+ to 0^+ [7] are evident as are the previously identified $10_1^+ \rightarrow (8_2^+)$ and $(8_2^+) \rightarrow 6_1^+$ transitions [20] at 745 and 347 keV, respectively. The efficiency corrected ratio for the intensity of the 660, 814, 906, and 994 keV transitions compared to the 96 keV transition is 2.7(1) giving an IC coefficient for the 96 keV transition of 1.7(1), in excellent agreement with both previous measurements [20,21] and the theoretical prediction for an $E2$ transition of 1.62(7) obtained using the program BRICC [29]. The γ-ray branching ratio of the 10^+ state to the nonyrast (8^+) state was found to be 9(1)% by comparing the mean intensity of the 347 and 745 keV peaks to that of the 1092 keV peak.

Figure 2 clearly shows peaks at 267 and 408 keV. These transitions have been seen before [7,8] and tentatively assigned

as the $(16^+) \to (15^+)$ and $(15^+) \to 14^+$ transitions, respectively. The right inset of Fig. 2 indicates the presence of two further transitions. The weaker 1545 keV peak was identified in the ^{94}Ag β-decay studies and provisionally assigned as the $(18^+) \to (16^+)$ decay, but the more intense 1651 keV transition was not seen. The left inset of Fig. 2 shows evidence of a small peak at 106 keV. The agreement between the summed intensity of the 1545 and 1651 keV transitions and the individual intensities of the 267 and 408 keV transitions is excellent once detector efficiency has been accounted for. The final transition previously identified above the 14^+ state had an energy of 597 keV [7,8]. This is not seen in the present data.

Figures 3(a) and 3(b) show the low-energy part of the coincidence spectra for the 1545 and 1651 keV transitions. The coincidence gate used to produce the γ-γ matrix required that γ rays were seen between $t = 100$ and $t = 800$ ns. In both cases the 267 and 408 keV peaks can be seen. However, the 1545 coincident spectrum has a further peak at 106 keV. The
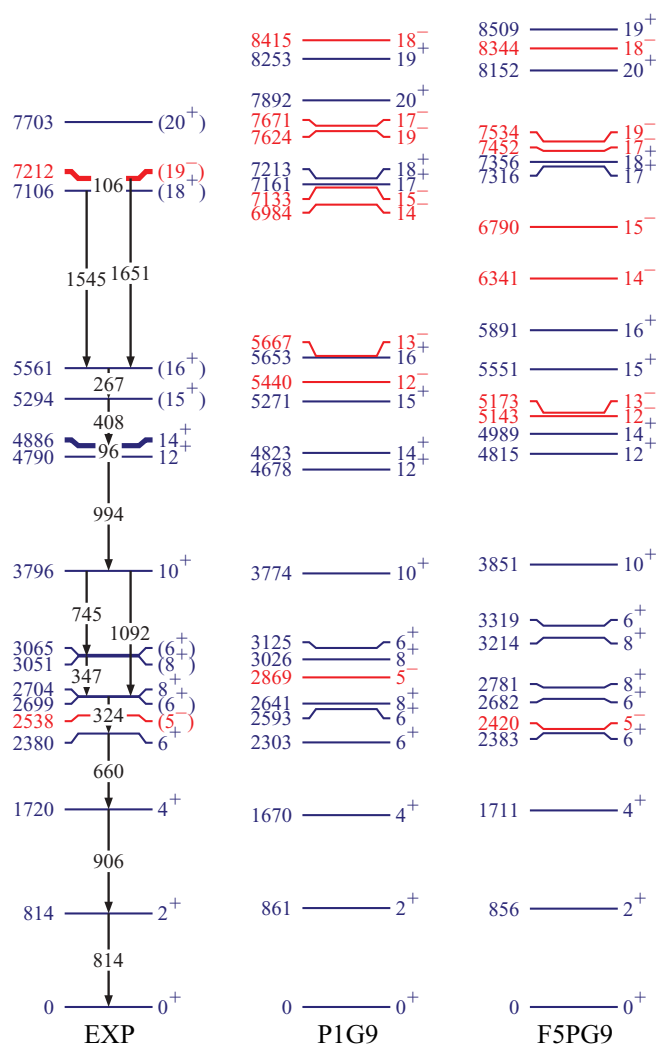
same peak is seen in coincidence with the 267 and 408 keV transitions [Figs. 3(c) and 3(d)].

From the above, and the lack of any other clear transitions seen in singles or coincidence, we conclude that ^{94}Pd has a second isomer at 7212 keV that can decay through two channels, a 1651 keV transition to the (16^+) state or a 106 keV transition to the (18^+) state, as shown in the left part of Fig. 4. The experimental results for the isomers are summarized in Table I. The data unambiguously places the 1545 keV transition above the 408 and 267 keV transitions and below the 597 keV transition in the ^{94}Pd level scheme, an assignment that was previously based only on shell-model calculations and comparison with the $N = 48$ isotones [8]. However, the ordering of the 267 and 408 keV transitions still remains uncertain.

The size of the Compton background makes isomer half-life measurements using the low-energy γ rays at 267 and 408 keV difficult. Conversely, the background under the 1545 and 1651 keV peaks can have no direct contribution from Compton scattering of photons from the transitions below the 14^+ isomer; the prompt flash is also small and well constrained due to optimal time resolution at these energies. For the 1545 keV transition it is the low statistics which does not allow for a reliable half-life measurement. However, it was possible to implement a background-subtracted, weighted-least-squares exponential fit to the time distribution of counts in the 1651 keV peak, as shown in the bottom left corner of Fig. 5. This gave a value of 197(22) ns.

For the transitions below the 14^+ isomer in ^{94}Pd, the statistics are much higher. The top of Fig. 5 shows the time distribution for this isomer derived from the present work. Here the only events considered were those in which at least two γ rays are seen with energies corresponding to transitions in the yrast cascade from $12^+ \to 0^+$ (the 96 keV transition is omitted due to the poor time resolution at this energy). The time spectrum was then incremented with the time of the highest energy γ ray seen from the cascade if all the transitions seen from the cascade fell within a coincidence window of 250 ns. The line shown in the figure is a single-component exponential fit with no background subtraction, using only

FIG. 4. (Color online) Experimental (left) and calculated energy levels (see text for details) of ^{94}Pd. The tentative spin and parity assignment for the new isomer at 7212 keV is based on the current work. Assignments for other states are based on prior results [7,8,17,20]. Only transitions observed in the current work are shown.
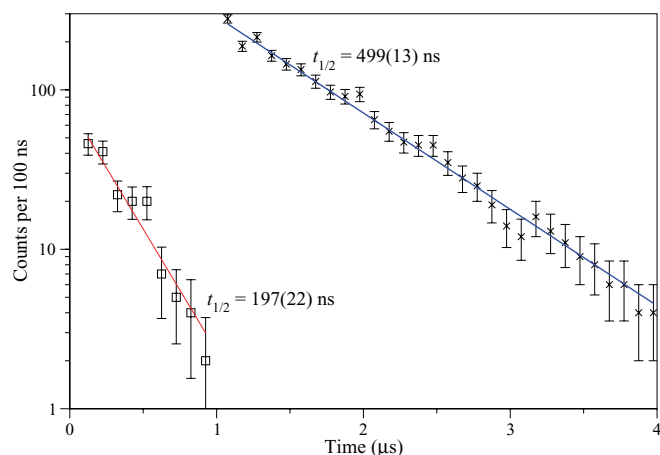

FIG. 5. (Color online) Decay curve for the 1651 keV transition (open squares) and for transitions below the 14^+ isomer (crosses) (see text).

TABLE I. Experimental decay energies, half lives, branching ratios (BR) and transition rates for the assigned electric multipoles of order L (EL) together with F5PG9 calculations of transition rates for the isomers in ^{94}Pd. "F5PG9-a" uses effective charges of 1.72/1.44e for protons/neutrons while "F5PG9-b" uses 1.5/0.5e.

E_{level} (keV)	Half-life (ns)	E_γ (keV)	BR (%)	$I^\pi_{initial} \rightarrow I^\pi_{final}$	EL	B (EL) (W.u.) Expt.	F5PG9-a	F5PG9-b
7212	197(22)	1651	80(4)	$(19^-) \rightarrow (16^+)$	$E3$	0.28(4)	0.18	0.10
		106	20(4)[a]	$(19^-) \rightarrow (18^+)$	$E1$	$3(1)\times10^{-7}$		
				$19^- \rightarrow 17^-$	$E2$		9.74	5.52
4886	499(13)	96	100[a]	$14^+ \rightarrow 12^+$	$E2$	2.1(1)[b]	5.49	2.69

[a]Including internal conversion.

[b]Assuming a γ-ray energy of exactly 96 keV and IC coefficient of 1.62.

data with $t > 1$ μs. Given the measured half-life of the new isomer and its relatively low population, this fit should be characteristic of only the 14^+ isomer. From this we infer a value of 499(13) ns for this state, which is intermediate between the values of Grzywacz [530(10) ns [19]] and Garnsworthy *et al.* [468(19) ns [21]]. The reliability of the assumption of vanishing background in this analysis is confirmed by the excellent agreement with fits to the time spectra resulting from gates on individual peaks *with* background subtraction.

Assuming the prior spin/parity assignments of the state at 5561 keV to be correct (see below), Weisskopf estimates would seem to give only one reasonable option for the spin of the state of the new isomer, namely, 19. A lower spin would open the possibility of fast quadrupole decays; with a higher spin, one should expect a millisecond (or longer) half-life for a 1651 keV γ decay to a 16^+ state. Assigning the above spin, the reduced $E3$ and $M3$ transition strengths are 0.28 and 12 W.u., respectively. The latter exceeds the recommended upper limit for such a transition given in Ref. [30] by 20%. The corresponding $E1$ and $M1$ Weisskopf strengths for a 106 keV transition are 0.3 and 10 μW.u., respectively. Again the data would appear to support a transition of electric character, with retarded $E1$ transitions as low as 10^{-7} W.u. being fairly common, while $M1$ transitions with strengths of 10^{-5} W.u. are less so [30]. Hence we tentatively assign a spin and parity of 19^- to the new isomer.

In order to compare results with theoretical expectations, two different SM calculations were carried out using the code OXBASH [31]. The first—henceforth known as P1G9 and illustrated in the center of Fig. 4—used only the empirical shell-model interaction of Gross and Frenkel [4] (GF) in the $\pi\nu(p_{1/2}, g_{9/2})$ model space. This is a fit to experimental level schemes and binding energies and extrapolates proton and neutron single-hole energies (SHE) to ^{100}Sn. This is the same calculation as found in Fig. 5(b) of Ref. [7] but here we include several additional states. The second—referred to as F5PG9 and shown at the right of Fig. 4—is based on the same interaction for the $\pi\nu(p_{1/2}, g_{9/2})$ model space but was augmented by the $\pi\nu(f_{5/2}, p_{3/2})$ model space using an interaction derived from the CD-Bonn nucleon-nucleon potential [32]. Core polarization has been corrected for following the many-body approach outlined in Ref. [33] assuming a ^{56}Ni core, with the two-body matrix elements (TBME) scaled down by $(\frac{56}{100})^{1/3}$. This interaction was tuned to reproduce the experimental $p_{3/2}$ and $f_{5/2}$ SHE in ^{88}Sr

and the extrapolated SHE for all valence orbits in ^{100}Sn [34]. As the GF interaction was empirically fitted to the restricted model space, it has to be corrected for the extended space to avoid "double counting" of interaction strength which is most severe in the $T = 1$ pairing channel. Therefore, all $I^\pi = 0^+$ GF TBME were reduced by 540 keV, keeping the multiplet monopole unchanged. Moreover, all nondiagonal TBME in the GF space were reduced to 50%. Transition rates were calculated using typical effective charges for the GF space of 1.72e and 1.44e [5] and alternatively 1.5e and 0.5e for protons and neutrons, respectively. For $E2$ transitions, the latter might be more appropriate for the extended F5PG9 model space which allows $E3$ and $M2$ transitions, while $E1$ is still excluded.

In both calculations the yrast states up to the 14^+ isomer are well reproduced. Above this isomer, the first question relates to the ordering and spin-parities of the states decaying via the 267 and 408 keV γ rays. In both cases the 15^+ and 16^+ states are the only states that seem reasonable with gaps in excess of 1500 keV between the 16^+ state and the next positive-parity state, while the negative-parity states are nonyrast by several hundred kilo-electron-volts. In the F5PG9 model space, the gap between the 15^+ and 16^+ states has decreased, while the 14^+ to 15^+ gap has increased, which matches the adopted order of the 408 and 267 keV transitions better than the P1G9 calculation. It is, however, the original P1G9 calculations that better match experiment for the absolute excitation energy of the proposed 16^+ state. It should be noted here that the P1G9 calculations reproduce the evolution of the $N = 48$ yrast states very well with the exception of the (16^+) in ^{92}Ru, where the (16^+_2) state seems to better fit the systematics (see Ref. [8], and references therein).

The most notable difference between the two models is the lowering of the negative-parity states with the inclusion of np-nh excitations from the negative-parity $f_{5/2}$ and $p_{3/2}$ orbitals. This yields better agreement for the excitation energy of the lowest 5^- state compared to the original P1G9 calculation though the reduction in energy is slightly too large. The sequence of high-spin states of both parities is generally well reproduced in both approaches, the key exception being the reversed order of the 17^- and 19^- states in the F5PG9 calculation, the former of which is lower in energy by about 80 keV. This is within the uncertainty of the shell-model prediction and possibly due to insufficient correction of the "double counting" of interaction strength and/or the lack of

inclusion of excitations across the $N = 50$ shell gap. The latter was seen to be important in reproducing the isomerism of the (21^+) state in ^{94}Ag [8,13]. In the P1G9 calculation, the 19^- state has a pure $(\pi p_{1/2}^{-1} g_{9/2}^{-3})_{11} \otimes (\nu g_{9/2}^{-2})_8$ configuration and corresponds to the maximum-spin negative-parity state allowed in the space; in the F5PG9 calculation this remains the dominant configuration (89.5%) but is supplemented by small admixtures of $(\pi p_{3/2}^{-1} g_{9/2}^{-3}) \otimes (\nu g_{9/2}^{-2})$ (6.3%) and $(\pi f_{5/2}^{-1} g_{9/2}^{-3}) \otimes (\nu g_{9/2}^{-2})$ (4.0%).

An alternative interpretation for the isomerism—that the state at 7212 is actually a 17^- state that is fed by an unseen, isomeric, low-energy, highly converted transition from a higher lying 19^- state—cannot be firmly ruled out from the data. However, the comparable branching ratios for the transitions from the state at 7212 keV to the states at 5561 and 7106 keV seems improbable for transitions that are of the same multipolarity but differ by an order of magnitude in energy. Since this argument would apply even if the state at 7106 were the 17^+ state and both calculations support the assignment of 16^+ for the state at 5561 keV, we discount this possibility.

SM-reduced transition strengths for observed and predicted (but not observed) transitions are listed in Table I for the two choices of effective charges. It appears that the $14^+ \rightarrow 12^+$ strength is better reproduced by the smaller polarization charge which is partly due to the extended model space. The $19^- \rightarrow 16^+$ E3 transition is mainly a proton $g_{9/2} \rightarrow p_{3/2}$ stretched $\Delta I = \Delta l = 3$ transition which is better reproduced by a larger effective charge. A similar feature has been observed in higher major shells above ^{132}Sn and ^{208}Pb for ^{134}Te and ^{210}Po for corresponding $h_{11/2} \rightarrow d_{5/2}$ and $i_{13/2} \rightarrow f_{7/2}$ transitions [35].

In summary, a new high-spin isomeric state with a half-life of 197(22) ns has been discovered in the $N = Z + 2$ nuclide ^{94}Pd. We tentatively assign it as a (19^-) state with dominant configuration $(\pi p_{1/2}^{-1} g_{9/2}^{-3})_{11} \otimes (\nu g_{9/2}^{-2})_8$ and both E1 and E3 decay branches. The present results reveal the importance of including the well-bound $f_{5/2}$ and $p_{3/2}$ orbits for understanding the decay properties of high-spin isomers in the vicinity of ^{100}Sn. Such isomers and their decay properties provide an excellent testing ground for empirical interactions and model spaces and form an important step in the development and understanding of proton-neutron interactions in nuclei.

[1] H. Schatz *et al.*, Phys. Rep. **294**, 167 (1998).
[2] H. Grawe and M. Lewitowicz, Nucl. Phys. A **693**, 116 (2001).
[3] H. Grawe, in *Euroschool Lectures on Physics with Exotic Beams*, edited by J. Al-Khalili and E. Roeckl, Springer Lecture Notes in Physics, Vol. 1 (Springer, Berlin, 2004), p. 33.
[4] R. Gross and A. Frenkel, Nucl. Phys. A **267**, 85 (1976).
[5] D. Rudolph, K. Lieb, and H. Grawe, Nucl. Phys. A **597**, 298 (1996).
[6] H. Grawe, A. Blazhev, M. Górska, R. Grzywacz, H. Mach, and I. Mukha, Eur. Phys. J. A **27**, SO1, 257 (2006).
[7] M. La Commara *et al.*, Nucl. Phys. A **708**, 167 (2002).
[8] C. Plettner *et al.*, Nucl. Phys. A **733**, 20 (2004).
[9] I. Mukha *et al.*, Phys. Rev. C **70**, 044311 (2004).
[10] I. Mukha *et al.*, Phys. Rev. Lett. **95**, 022501 (2005).
[11] I. Mukha *et al.*, Nature (London) **439**, 298 (2006).
[12] O. L. Pechenaya *et al.*, Phys. Rev. C **76**, 011304(R) (2007).
[13] K. Kaneko, Y. Sun, M. Hasegawa, and T. Mizusaki, Phys. Rev. C **77**, 064304 (2008).
[14] A. Kankainen *et al.*, Phys. Rev. Lett. **101**, 142503 (2008).
[15] J. Cerny, D. M. Moltz, D. W. Lee, K. Peräjärvi, B. R. Barquest, L. E. Grossman, W. Jeong, and C. C. Jewett, Phys. Rev. Lett. **103**, 152502 (2009).
[16] D. G. Jenkins, Phys. Rev. C **80**, 054303 (2009).
[17] M. Górska *et al.*, Z. Phys. A **353**, 233 (1995).
[18] R. Grzywacz *et al.*, Phys. Rev. C **55**, 1126 (1997).
[19] R. Grzywacz, in ENAM 98, *Exotic Nuclei and Atomic Masses*, edited by B. M. Sherill, D. J. Morrissey, and C. N. Davids (AIP, Woodbury, NY, 1998), p. 430.
[20] N. Mărginean *et al.*, Phys. Rev. C **67**, 061301(R) (2003).
[21] A. B. Garnsworthy *et al.*, Phys. Rev. C **80**, 064303 (2009).
[22] H. Geissel *et al.*, Nucl. Instrum. Methods Phys. Res. A **70**, 286 (1992).

[23] S. Pietri *et al.*, Nucl. Instrum. Methods Phys. Res. A **261**, 1079 (2007).
[24] R. Kumar *et al.*, Nucl. Instrum. Methods Phys. Res. **598**, 754 (2009).
[25] R. Brun and F. Rademakers, ROOT — An Object Orientated Data Analysis Framework, Proceedings AIHENP'96 Workshop, Lausanne, Sep. 1996, Nucl. Instrum. Methods Phys. Res. A **389**, 81 (1997), See also [http://root.cern.ch/].
[26] D. Radford, Nucl. Instrum. Methods Phys. Res. A **361**, 297 (1995).
[27] F. James, MINUIT: Function Minimization and Error Analysis Reference Manual, CERN, CERN Geneva, Switzerland, version 94.1 ed. (2000), CERN Program Library Long Writeup D506.
[28] Zs. Podolyák *et al.*, Nucl. Phys. A **722**, C273 (2003).
[29] T. Kibédi, T. Burrows, M. Trzhaskovskaya, P. Davidson, and C. W. Nestor Jr., Nucl. Instrum. Methods Phys. Res. A **589**, 202 (2008).
[30] P. Endt, At. Data Nucl. Data Tables **26**, 47 (1981).
[31] B. Brown, A. Etchegoyen, N. Godwin, W. Rae, W. Richter, W. Ormand, E. Warburton, J. Winfield, L. Zhao, and C. Zimmerman, OXBASH for Windows, MSU-NSCL Report No. 1289, 2004.
[32] R. Machleidt, Phys. Rev. C **63**, 024001 (2001).
[33] M. Hjorth-Jensen, T. Kuo, and E. Osnes, Phys. Rep. **261**, 125 (1995).
[34] H. Grawe, K. Langanke, and G. Martínez-Pinedo, Rep. Progr. Phys. **70**, 1525 (2007); H. Grawe, R. Schubart, K. H. Maier, D. Seweryniak, and OSIRIS/NORDBALL Collaborations, Phys. Scr. T **56**, 71 (1995).
[35] J. P. Omtvedt, H. Mach, B. Fogelberg, D. Jerrestam, M. Hellström, L. Spanier, K. I. Erokhina, and V. I. Isakov, Phys. Rev. Lett. **75**, 3090 (1995).